

APPLICATION OF LASER-PLASMA ACCELERATOR BEAMS TO FREE-ELECTRON LASERS*

C.B. Schroeder, C. Benedetti, E. Esarey, W.P. Leemans, J. van Tilborg,
LBNL, Berkeley, CA 94720, USA

Y. Ding, Z. Huang, SLAC, Menlo Park, CA 94025, USA

F.J. Grüner, A.R. Maier, CFEL, 22607 Hamburg, Germany

Abstract

Laser-plasma accelerators are able to produce ultra-high accelerating fields, enabling compact accelerators, and ultra-short (fs) beams with high-peak currents. We review recent progress on the development of laser-plasma accelerators and, in particular, recent measurements characterizing the properties of an electron beam generated by a laser-plasma accelerator. It is shown that the 6D beam brightness of a laser-plasma accelerated beam is comparable to state-of-the-art conventional electron beam sources. Given present experimentally achievable laser-plasma accelerator electron beam parameters, we discuss beam decompression as a method of realizing a laser-plasma-accelerator-based free-electron laser.

INTRODUCTION

Laser-plasma accelerators (LPAs) have attracted considerable attention owing to their ability to generate ultra-high accelerating gradients, enabling compact accelerators. Laser-plasma acceleration is realized by using a high-intensity laser to ponderomotively drive a large plasma wave (or wakefield) in an underdense plasma [1]. The plasma wave has relativistic phase velocity, and can support large electric fields in the direction of the laser propagation. When the laser pulse is approximately resonant (pulse duration on the order of the plasma period) and the laser intensity is relativistic, with normalized laser vector potential $a = eA/m_e c^2 \sim 1$, the size of the accelerating field supported by the plasma is on the order of $E_0 = m_e c \omega_p / e$, or $E_0 [\text{V/m}] \simeq 96 \sqrt{n_0} [\text{cm}^{-3}]$, where $\omega_p = k_p c = (4\pi n_0 e^2 / m_e)^{1/2}$ is the electron plasma frequency, n_0 is the ambient electron number density, m_e and e are the electronic mass and charge, respectively, and c is the speed of light in vacuum. For example, an accelerating gradient of ~ 100 GV/m is achieved operating at a plasma density of $n_0 \sim 10^{18} \text{ cm}^{-3}$. Owing to these ultra-high accelerating gradients LPAs are actively being researched as compact sources of energetic beams for light sources [2, 3, 4, 5] and future linear colliders [6].

In addition to extremely large accelerating gradients, plasma-based accelerators intrinsically produce ultra-short (fs) electron bunches that are a fraction of the plasma wavelength $\lambda_p = 2\pi/\omega_p$ or $\lambda_p [\text{m}] = 3.3 \times 10^4 / \sqrt{n_0} [\text{cm}^{-3}]$. Because of the short beam durations, LPAs are sources

of high peak current beams (~ 1 – 10 kA), and, hence, it is natural to consider LPA electron beams as drivers for a free-electron laser (FEL) producing high-peak brightness radiation. LPA electron beams have been coupled into undulators to produce undulator radiation in the visible [7] and soft-x-ray [8]. In this proceedings paper we consider the prospects for applying LPA electron beams to drive an FEL.

LASER-PLASMA ACCELERATOR BEAM PHASE SPACE

High-quality electron beams up to ~ 1 GeV have been experimentally demonstrated using 40 TW lasers interacting in centimeter-scale plasma channels [9, 10]. Figure 1 shows a single-shot spectra of a 500 MeV electron beam generated using the LPA at LBNL. In Fig. 1 a 1.5 J, 0.8- μm laser interacts with a 225 μm diameter H-discharge capillary with on-axis density $3.5 \times 10^{18} \text{ cm}^{-3}$. The H-discharge capillary forms a plasma channel for guiding the laser. LPAs are capable of compactly producing 0.5 GeV beams with tens of pC of charge, few percent-level relative energy spread, and mrad divergences, and here we will consider such a beam for driving an FEL.

Recent experimental effort in the plasma-based accelerator community has been focused on improved diagnostics and measurements of the LPA electron beam phase space, and, in particular, measurements of the beam transverse emittance and the beam duration.

Transverse Emittance

The beam transverse size in the plasma wave can be determined by measuring the spectrum of betatron x-rays produced by the beam in the plasma wave [11, 12, 13]. The electron beam undergoes betatron motion in the strong focusing forces ($F_{\perp} \sim eE_0 k_p r$) of the plasma wave, and emits fs, hard x-rays [14]. The effective wiggler strength parameter $a_{\beta} = \gamma_z k_{\beta} r_{\beta}$ is typically large $a_{\beta} \gg 1$ (where γ_z is the Lorentz factor of the longitudinal momentum, k_{β} the betatron wavenumber, and r_{β} the amplitude of the electron betatron orbit), and the x-ray spectrum is broad. The spectrum is characterized by the critical frequency $\omega_c \simeq 3a_{\beta} \gamma_z^2 k_{\beta} c \propto \gamma_z^2 n_0 r_{\beta}$. Owing to the strength of the transverse focusing force in the plasma wave, the beam emits hard x-rays (~ 10 keV). By measuring the spectrum (i.e., ω_c), the amplitude of the betatron oscillation r_{β} (i.e., the beam radius) may be estimated. This measurement is a non-invasive, in situ, single-shot diagnostic of the

*Work supported by the Director, Office of Science, of the U.S. Department of Energy under Contract No. DE-AC02-05CH11231, by the National Science Foundation under Grant and PHY-0917687.

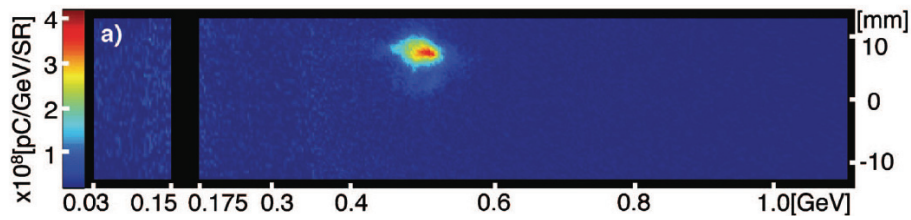


Figure 1: Single-shot electron beam spectrum from a $225 \mu\text{m}$ diameter H-discharge capillary with on-axis density $3.5 \times 10^{18} \text{ cm}^{-3}$ and a 1.5 J laser. The H-discharge capillary forms a plasma channel for guiding the laser. The 0.5 GeV electron beam contained 50 pc of charge, with 5.6% (rms) energy spread and 2 mrad (rms) divergence [10].

beam size and, combined with a divergence measurement, may be used to estimate the beam transverse emittance. This diagnostic was implemented at LBNL [13], where a 463 MeV beam was generated, with 2.8% (rms) energy spread and 1.2 mrad (rms) divergence, and the x-ray betatron spectrum was measured indicating a beam size of $0.1 \mu\text{m}$ and an estimated normalized transverse emittance of $\epsilon_n \lesssim \gamma\sigma_\theta\sigma_x \simeq 0.1 \text{ mm mrad}$.

Bunch Duration

The bunch duration of the LPA beam has recently been measured with fs resolution [15, 16]. Previous LPA bunch duration measurements were limited in resolution to tens of fs [17]. One technique uses the spectrum of coherent transition radiation (CTR), generated as the beam passed through a foil following the plasma, to determine beam temporal profile. Analysis of the CTR spectrum generated by the electron beams (produced using colliding pulse injection, as described below) indicated $\tau_b = 1.4 \text{ fs}$ (rms) bunches and a peak current of $I = 4 \text{ kA}$ [15].

LPA electron beam duration measurements have also been performed using an ultra-short optical probe [16]. In this single-shot, non-invasive, in-situ diagnostic, the azimuthal magnetic field generated by the beam was probed in the plasma using Faraday rotation. Here an ultra-short laser propagates orthogonal to the LPA electron beam propagation direction. The probe rays passing above and below the beam have their polarization rotated in opposite directions, and the beam duration is determined using time-resolved polarimetry. Using this technique the LPA beam (produced using self-trapping with a single laser pulse) duration was measured as $\tau_b = 5.8 \text{ fs}$ (FWHM) [16].

Controlled Injection

To control the LPA beam phase space characteristics and to improve the shot-to-shot stability and tunability of the beam parameters, research has focused on methods to provide detailed control of the injection of background plasma electrons into the plasma wave. One method to trigger injection into the plasma wave is to collide laser pulses in the plasma [19]. In this colliding pulse injection technique two lasers overlap in space and time, generating a localized beat wave that imparts momentum to the plasma electrons and enables trapping. This technique was experimentally real-

ized at LOA [20], where stable beams with energy spreads as low as 1% (FWHM) have been produced [21].

Another promising method is to rely on plasma density tailoring, where a short ($\sim \text{mm}$), high ($\sim 10^{19} \text{ cm}^{-3}$) plasma density region to serve as a localized plasma injector, is followed by a long ($\sim \text{cm}$), low ($\sim 10^{18} \text{ cm}^{-3}$) plasma density region to serve as a dark-current-free accelerator stage [22]. This approach relies on locally slowing the plasma wave phase velocity to facilitate trapping of background plasma electrons. The wave phase velocity is controlled via the plasma density gradient [23] and the increasing laser intensity [24] (generated by the relativistic self-focusing produced in the high plasma density region). Using density tailoring to control injection into a plasma accelerator was experimentally realized at LBNL by integrating a gas jet into a discharge capillary. Electron trapping and energy gain was controlled by varying the gas jet density and the laser focal position. This method of triggered injection produced greatly improved stability (percent-level) of the LPA beam properties [22].

Beam Brightness

With the recent measurements of the LPA beam characteristics, the 6D beam brightness of the LPA electron beam can be estimated. The 6D beam brightness may be defined as

$$B_{6D} = \frac{N}{\epsilon_{nz}\epsilon_{ny}\epsilon_{nx}} \approx \frac{(I/I_A)}{r_e\epsilon_n^2\sigma_\gamma} \equiv b_6\lambda_c^{-3}, \quad (1)$$

where I is the peak current, N the number of beam electrons, $mc^2\sigma_\gamma$ the energy spread, and ϵ_{nz} , ϵ_{ny} , ϵ_{nx} the normalized longitudinal and transverse emittances. Here $I_A = m_e c^3/e \simeq 17 \text{ kA}$ is the Alfvén current, $r_e = e^2/m_e c^2$ is the classical electron radius, and $\lambda_c = \lambda_c/2\pi$ with λ_c the Compton wavelength. For an LPA electron beam with typical parameters (e.g., 0.5 GeV, $I = 4 \text{ kA}$, $\epsilon_n = 0.1 \text{ mm mrad}$, and $\sigma_\gamma/\gamma = 0.04$), the normalized 6D brightness is $b_6 \approx 10^{-11}$. This 6D beam brightness is comparable to conventional accelerators. For example, the LCLS beam at SLAC, with 13.6 GeV, $\sigma_\gamma/\gamma = 10^{-4}$, $I = 3.4 \text{ kA}$, and $\epsilon_n = 0.4 \text{ mm mrad}$, has a normalized 6D beam brightness of $b_6 \approx 10^{-11}$.

FEL APPLICATION

The fundamental resonant wavelength emitted in the FEL is $\lambda = \lambda_u(1 + K^2/2)/2\gamma^2$, where λ_u is the undulator wavelength and K is the undulator strength parameter, and the basic scalings of the FEL are determined by the FEL parameter:

$$\rho = \frac{1}{4\gamma} \left[\frac{I}{I_A} \left(\frac{K[JJ]\lambda_u}{\pi\sigma_x} \right)^2 \right]^{1/3}, \quad (2)$$

with σ_x the beam transverse size, $[JJ] = [J_0(\chi) - J_1(\chi)]$ (planar undulator), $\chi = K^2(4 + 2K^2)^{-1}$, and J_m are Bessel functions. The gain length (e-folding length of the fundamental radiation power) is $L_g = \lambda_u/4\pi\sqrt{3}\rho$ (neglecting diffraction, energy spread, and emittance effects).

The FEL requires the relative slice (i.e., over a coherence length $L_c = \lambda L_g/\lambda_u$) energy spread to be less than the FEL parameter $\sigma_\gamma/\gamma < \rho$. Satisfying this requirement has been a challenge for LPA-generated electron beams, which typically have relative energy spreads on the percent-level. The effect of energy spread on the FEL gain length can be estimated as $L_g(\sigma_\gamma)/L_g(\sigma_\gamma = 0) \approx [1 + (\sigma_\gamma/\gamma)^2/\rho^2]$. Although controlled injection techniques are actively being researched to reduce the LPA beam energy spread, the percent-level energy spreads that are presently demonstrated experimentally have hindered FEL applications.

Slippage in the FEL is also a major concern for LPA-driven FELs operating in the soft x-ray (or longer wavelengths) given the ultra-short (fs) bunch durations. It is desirable for the beam length to be longer than the slippage during propagation through the undulator $N_u\lambda \sim \lambda/\rho < L_b$. Typically $\lambda/\rho > L_b$ for an LPA-driven FEL operating in the soft-x-ray regime.

Although the 6D beam brightness is comparable to conventional sources, the LPA beam phase space distribution is not optimized for the FEL application. If we consider an XUV (e.g., tens of nm wavelength) FEL driven by a 0.5 GeV LPA beam (see, for example, the design study in Ref. [3]), the LPA projected beam energy spread is an order of magnitude larger than the FEL parameter $\rho \sim 5 \times 10^{-3} - 10^{-2}$. Although there are indications that the LPA beam slice energy spread may be significantly lower ($\sim 0.5\%$) than the projected [18], the LPA bunch length is on the order of the coherence length $L_b \sim L_c \sim 1 \mu\text{m}$ (i.e., the beam is a single slice).

There are several possible paths to realizing an FEL using experimentally demonstrated LPA electron beams. One possibility is simple energy collimation of the beam (e.g., using a chicane and a slit) to reduce the relative energy spread. Another possibility is to decompress the beam. Decompression has the advantage of potentially mitigating both the large energy spread and slippage effects. Stretching of an initially energy chirped beam was considered in Ref. [25]. A third possibility is to produce a correlation between energy and transverse position, and then to use a

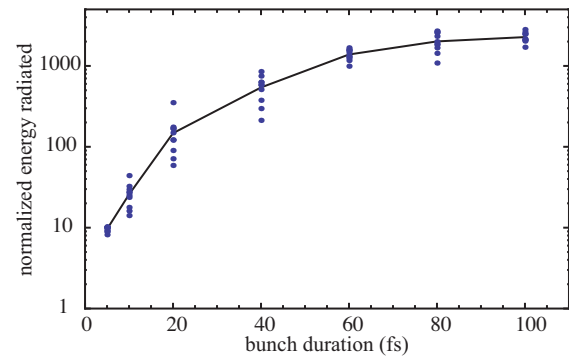


Figure 2: Normalized FEL radiation energy versus bunch duration (after decompression). The dots show different beam shot noise seeds, and the solid line is the mean.

transverse gradient undulator to satisfy the resonant condition for all energies [26]. Although requiring a more complicated canted-pole undulator design, the use of a transverse gradient undulator has potentially a number of advantages, including generation of ultrashort radiation, removing wavelength fluctuations due to beam energy jitter, reduced bandwidth (compared to decompression), and allowing seeding. In the next section we consider beam decompression. Further discussion of using a transverse gradient undulator can be found in Ref. [26].

BEAM DECOMPRESSION

A possible path to realizing an XUV or soft-x-ray FEL driven by an LPA, with experimentally demonstrated LPA beam parameters, is to decompress the LPA electron beam (e.g., by a factor of ~ 10 to a duration approximately the slippage distance in the FEL $L_b \sim \lambda/\rho$). The decompression will reduce the peak current, and, hence, the FEL parameter $\rho \propto I^{1/3}$. But, since the FEL parameter scales weakly with current, sufficient decompression will reduce the instantaneous energy spread to $\lesssim \rho$, providing a path for FEL lasing at soft-x-ray wavelengths.

Consider decompression of the beam by a factor $D > 1$, such that the bunch length increases to $\approx DL_b$, hence, the FEL parameter is reduced $\approx \rho D^{-1/3}$, and the instantaneous energy spread decreases to $\approx \sigma_\gamma/D$. The relative energy spread will be equal to the FEL parameter by decompressing such that $D = (\sigma_\gamma/\gamma\rho)^{3/2}$. The (1D) gain length after decompression can be estimated as

$$L_g \approx \frac{\lambda_u}{4\pi\sqrt{3}\rho} D^{1/3} \left[1 + D^{-4/3} \left(\frac{\sigma_\gamma}{\gamma\rho} \right)^2 \right]. \quad (3)$$

Equation (3) indicates the gain length is minimized $L_{g,\min} = (4/3^{3/4})(\sigma_\gamma/\gamma\rho)^{1/2}(\lambda_u/4\pi\sqrt{3}\rho)$ for $D = 3^{3/4}(\sigma_\gamma/\gamma\rho)^{3/2}$.

As a numerical example, consider an LPA-generated 0.5 GeV, 5 fs (FWHM), 50 pC electron beam, with 4% (rms) relative energy spread and 0.1 mm mrad transverse normalized emittance, coupled ($\sigma_x \simeq 20 \mu\text{m}$) to the

THUNDER undulator (2.18 cm period, $K = 1.85$, and $N_u = 220$ periods) [27] at LBNL. The fundamental wavelength radiated by the 0.5 GeV beam is $\lambda = 31$ nm. Figure 2 shows the normalized SASE FEL energy radiated by the beam versus bunch duration after propagation through the undulator. Figure 2 was generated using the code GINGER [28], where we have assumed a flat-top current profile, and the initially 5 fs beam is stretched using a chicane to produce a long (energy chirped) beam with reduced slice energy spread. The dots indicated different beam shot noise seeds, and the solid line is the mean. For these parameters the slippage time is $N_u \lambda / c \approx 23$ fs, and the relative energy spread equals the FEL parameter at ≈ 25 fs. Equation (3) predicts optimal decompression with $D \simeq 12$. Note that the Fig. 2 assumes a fixed undulator length, and none of the cases shown reach saturation. As indicated by Fig. 2, approximately two orders of magnitude improvement in FEL output can be achieved by bunch decompression, for these LPA electron beam and undulator parameters.

SUMMARY AND DISCUSSION

LPAs are able to generate high-quality electron beams with hundreds of MeV to GeV energies in several centimeters of plasma [9, 10]. It should be noted that, although the active acceleration region is cm-scale, the laser system typically occupies an area of tens of m^2 . LPA electron beams contain tens of pC of charge with fs durations [15, 16], and hence are of interest for high-peak current, ultrafast, light source applications. Recent measurements using betatron spectra have indicated an LPA beam transverse normalized emittance of ~ 0.1 mm mrad [13], less than that produced in conventional RF photocathodes.

Triggered injection is required to control the LPA electron beam phase space characteristics and to improve the shot-to-shot stability and tunability of the beam parameters. Several methods of triggered injection are actively being researched, including colliding pulse injection [19, 20, 21] and plasma density tailoring [22, 23].

The LPA 6D beam brightness is comparable to conventional sources, although the percent-level relative energy spreads and ultra-short bunch durations hinder FEL applications. One possible path to realization of an LPA-driven soft-x-ray FEL with experimentally demonstrated LPA beam parameters is to decompress the LPA beam such that the energy spread over a coherence length is $\lesssim \rho$, and the bunch length is $L_b \gtrsim \lambda / \rho$.

In addition to generating high-peak brightness LPA electron beams, a single laser system may drive multiple beamlines, producing ultra-short radiation from high-field THz to Thomson-scattered gamma rays [29], all intrinsically synchronized to the high-peak power drive laser. Future LPA experiments using more energetic (tens of Joules), short-pulse (tens of fs), PW laser systems [30] will enable generation of 10 GeV electron beams in less than a meter of plasma, opening the possibility of a compact LPA-driven hard-x-ray FEL.

ACKNOWLEDGMENTS

The authors would like to thank W. Fawley, R. Lindberg, S. Rieche, and K. Robinson for many enlightening discussions on the application of LPA beams to FELs.

REFERENCES

- [1] E. Esarey, C.B. Schroeder, and W.P. Leemans, *Rev. Mod. Phys.* 81 (2009) 1229.
- [2] F.J. Grüner et al., *Appl. Phys. B* 86 (2007) 431.
- [3] C.B. Schroeder et al., "Free-electron laser driven by the LBNL laser-plasma accelerator," AAC Workshop, Santa Cruz, July 2008, in *Advanced Accelerator Concepts*, AIP Proc. vol. 1086 (AIP, New York, 2009) p. 637.
- [4] C.B. Schroeder et al., "DESIGN OF AN XUV FEL DRIVEN BY THE LASER-PLASMA ACCELERATOR AT THE LBNL LOASIS FACILITY," FEL06, Berlin, 2006, p. 455, <http://www.JACoW.org>
- [5] D.A. Jaroszynski et al., *Philos. Trans. R. Soc. London, Ser. A* 364 (2006) 689.
- [6] C.B. Schroeder et al., *Phys. Rev. ST-Accel. Beams* 13 (2010) 101301.
- [7] H.-P. Schlenvoigt et al., *Nature Physics* 4 (2008) 130.
- [8] M. Fuchs et al., *Nature Physics* 5 (2009) 826.
- [9] W.P. Leemans et al., *Nature Physics* 2 (2006) 696.
- [10] K. Nakamura et al., *Phys. Plasmas* 14 (2007) 056708.
- [11] M. Schnell et al., *Phys. Rev. Lett.* 108 (2012) 075001.
- [12] S. Kneip et al., *Phys. Rev. ST-Accel. Beams* 15 (2012) 021302.
- [13] G. Plateau et al., *Phys. Rev. Lett.* 109 (2012) 064802.
- [14] E. Esarey et al., *Phys. Rev. E* 65 (2002) 056505.
- [15] O. Lundh et al., *Nature Physics* 7 (2011) 219.
- [16] A. Buck et al., *Nature Physics* 7 (2011) 543.
- [17] J. van Tilborg et al., *Phys. Rev. Lett.* 96 (2006) 014801.
- [18] C. Lin et al., *Phys. Rev. Lett.* 108 (2012) 094801.
- [19] E. Esarey et al., *Phys. Rev. Lett.* 79 (1997) 2682.
- [20] J. Faure et al., *Nature* 444 (2006) 737.
- [21] C. Rechatin et al., *Phys. Rev. Lett.* 102 (2009) 164801.
- [22] A.J. Gonsalves et al., *Nature Physics* 7 (2011) 862.
- [23] S.V. Bulanov et al., *Phys. Rev. E* 58 (1998) R5257.
- [24] C.B. Schroeder et al., *Phys. Rev. Lett.* 106 (2011) 135002.
- [25] A.R. Maier et al., *Phys. Rev.* (submitted).
- [26] Z. Huang et al., *Phys. Rev. Lett.* (submitted); SLAC-PUB-15193.
- [27] K. Robinson et al., *IEEE Journal of Quan. Electro.* 23 (1987) 1497.
- [28] W. M. Fawley, Technical Report LBNL-49625, Lawrence Berkeley National Laboratory (2002).
- [29] W.P. Leemans et al., *IEEE Trans. Plasma Sci.* 33 (2005) 8.
- [30] W.P. Leemans et al., "The BERkeley Lab Laser Accelerator (BELLA): A 10 GeV Laser Plasma Accelerator," AAC Workshop, Annapolis, MD, June 2010, in *Advanced Accelerator Concepts*, AIP Proc. vol. 1299 (AIP, New York, 2010) p. 3.